Protein Science (1995), *4*:671-680. Cambridge University Press. Printed in the USA.

An NMR and spin label study of the effects of binding calcium and troponin I inhibitory peptide to cardiac troponin C

JACK W. HOWARTH, GEORGE A. KRUDY,[1] XIN LIN, JOHN A. PUTKEY, AND PAUL R. ROSEVEAR

Department of Biochemistry and Molecular Biology, University of Texas Medical School-Houston, Houston, Texas 77225

(RECEIVED October 12, 1994; ACCEPTED February 7, 1995)

Abstract

The paramagnetic relaxation reagent, 4-hydroxy-2,2,6,6-tetramethylpiperidinyl-1-oxy (HyTEMPO), was used to probe the surface exposure of methionine residues of recombinant cardiac troponin C (cTnC) in the absence and presence of Ca^{2+} at the regulatory site (site II), as well as in the presence of the troponin I inhibitory peptide (cTnIp). Methyl resonances of the 10 Met residues of cTnC were chosen as spectral probes because they are thought to play a role in both formation of the N-terminal hydrophobic pocket and in the binding of cTnIp. Proton longitudinal relaxation rates (R_1's) of the [^{13}C-methyl] groups in [^{13}C-methyl]Met-labeled cTnC(C35S) were determined using a T_1 two-dimensional heteronuclear single- and multiple-quantum coherence pulse sequence. Solvent-exposed Met residues exhibit increased relaxation rates from the paramagnetic effect of HyTEMPO. Relaxation rates in $2Ca^{2+}$-loaded and Ca^{2+}-saturated cTnC, both in the presence and absence of HyTEMPO, permitted the topological mapping of the conformational changes induced by the binding of Ca^{2+} to site II, the site responsible for triggering muscle contraction. Calcium binding at site II resulted in an increased exposure of Met residues 45 and 81 to the soluble spin label HyTEMPO. This result is consistent with an opening of the hydrophobic pocket in the N-terminal domain of cTnC upon binding Ca^{2+} at site II. The binding of the inhibitory peptide cTnIp, corresponding to Asn 129 through Ile 149 of cTnI, to both $2Ca^{2+}$-loaded and Ca^{2+}-saturated cTnC was shown to protect Met residues 120 and 157 from HyTEMPO as determined by a decrease in their measured R_1 values. These results suggest that in both the $2Ca^{2+}$-loaded and Ca^{2+}-saturated forms of cTnC, cTnIp binds primarily to the C-terminal domain of cTnC.

Keywords: calcium; isotope labeling; paramagnetic relaxation; spin label; troponin C; troponin I peptide

Muscle contraction is regulated by the TnC component of the troponin complex. The troponin complex is made up of TnC, the Ca^{2+} regulatory subunit, TnI, the subunit that inhibits actomyosin ATPase activity, and TnT, the tropomyosin-binding subunit. Binding Ca^{2+} to TnC induces a conformational change, which is transmitted to TnI neutralizing the inhibition of the ATPase activity. TnC is a member of the helix-loop-helix or EF-hand family of Ca^{2+} binding proteins (Kretsinger, 1980). Crystallographic structures of sTnC reveal a dumbbell-shaped molecule with N- and C-terminal globular domains joined by a helical linker (Herzberg & James, 1985; Satyshur et al., 1988). Each domain contains two EF-hand Ca^{2+} binding sites. There are two isoforms of TnC; the fast skeletal muscle isoform, and the cardiac and slow skeletal muscle form. Although both isoforms have four potential Ca^{2+} binding sites, two high-affinity Ca^{2+}/Mg^{2+} sites (sites III and IV) and two low-affinity Ca^{2+}-specific sites (I and II), cTnC has a nonfunctional Ca^{2+} binding site I due to several critical amino acid substitutions (VanEerd & Takahashi, 1976; Collins et al., 1977). Sites III and IV located in the C-terminal domain and are largely responsible for maintaining the stability of TnC in the troponin complex (Zot & Potter, 1982; Negele et al., 1992). Calcium binding to site II, located in the N-terminal domain, has been shown to regulate muscle

Reprint requests to: Paul R. Rosevear, Department of Biochemistry and Molecular Biology, University of Texas Medical School-Houston, Houston, Texas 77225.

[1] Present address: Texas Biotechnology Corporation, 7000 Fannin Suite 1920, Houston, Texas 77030.

Abbreviations: TnC, cardiac or fast skeletal troponin C; cTnC, cardiac TnC; sTnC, fast skeletal TnC; cTnC3, recombinant cTnC(des M1, D2A); cTnC(C35S), recombinant cTnC(des M1, D2A; C35S); TnI, troponin I; cTnIp, cardiac troponin I inhibitory peptide corresponding to Asn 129 through Ile 149 of cTnI; sTnIp, skeletal troponin I inhibitory peptide corresponding to Gly 104 through Arg 115; Tris-d_{11}, deuterated tris(hydroxymethyl)amino-methane; HyTEMPO, 4-hydroxy-2,2,6,6-tetramethylpiperidinyl-1-oxy; HSMQC, two-dimensional heteronuclear single- and multiple-quantum coherence; MLCK, a 26-residue fragment of skeletal muscle myosin light chain kinase; CaM, calmodulin; TRNOE, transferred nuclear Overhauser effect; HMJ model, Herzberg, Moult, and James model.

contraction (Holroyde et al., 1980; Robertson et al., 1981; Putkey et al., 1989; Sweeney et al., 1990).

We have previously assigned the Met residues in recombinant cTnC, cTnC3 (Lin et al., 1994), and demonstrated the utility in using NMR and selective isotope labeling of Met residues in both cTnC and cTnI to probe protein–protein interactions central to muscle contraction (Krudy et al., 1994). Using [^{13}C-methyl]Met-labeled cTnC, all 10 cTnC Met residues could be resolved in the HSMQC spectrum of the cTnI–cTnC complex. The largest chemical shift changes in cTnC upon complex formation with cTnI were observed for Met 81, Met 120, and Met 157 (Krudy et al., 1994). Methionines 120 and 157 are located in the C-terminal domain of cTnC. These studies demonstrate the utility of selective isotope labeling of Met residues in cTnC to monitor conformational changes central to muscle contraction in the large cTnC–cTnI complex (40,000 Da). Previously, selective isotope labeling of Met residues has been used to detect and monitor ligand-induced conformational changes in proteins having an approximate molecular mass of 66,000 (Rosevear, 1988)

Modeling studies, based on the crystal structure of sTnC, have suggested that Ca^{2+}-induced exposure of hydrophobic sites in TnC results in an enhanced interaction with a Ca^{2+}-specific binding site on TnI (Herzberg et al., 1986). Specifically, the Herzberg, Moult, and James model suggests that Ca^{2+} binding to the N-terminal domain of TnC results in the movement of helices B and C away from helices A and D, forming a hydrophobic surface or pocket that has been suggested to provide the critical TnI interaction responsible for relieving the inhibition of the actomyosin ATPase (Herzberg et al., 1986; Strynadka & James, 1989). This model has recently received strong experimental support (Grabarek et al., 1990). However, the specific hydrophobic surface exposed in either TnC or TnI has not been defined. We have recently modeled the N-terminal domain of cTnC in the presence and absence of Ca^{2+} (Brito et al., 1991). Based on this structure, the HMJ model predicts that side chains of methionines 45, 80, and 81 are all exposed in the presence of bound Ca^{2+} at site II and at least partially buried in the absence of bound Ca^{2+}. In the present studies, we utilize a soluble paramagnetic spin label to probe the surface exposure of the 10 Met residues in both $2Ca^{2+}$-loaded and Ca^{2+}-saturated cTnC. Comparison of the experimentally determined changes in surface exposure of the Met residues upon Ca^{2+} binding at site II with those predicted provides a test of the HMJ model.

By comparison with CaM, Met residues in cTnC may also be involved in binding the cTnI inhibitory peptide (129–149), which corresponds to the well-known skeletal inhibitory peptide, TnI (96–115), of sTnI. Methionine residues 36, 71, 72, 76, and 145 in bovine CaM correspond to Met residues 45, 80, 81, 85, and 157 in cTnC, respectively. In CaM, Met residues 36, 51, 71, and 72 form a portion of the N-terminal hydrophobic patch with Met residues 109, 124, 144, and 145 forming a similar portion of the C-terminal hydrophobic patch (Babu et al., 1988; Taylor et al., 1991). Four Met residues in the C-terminal domain (Met 109, Met 124, Met 144, and Met 145) and four Met residues in the N-terminal domain (Met 36, Met 51, Met 71, and Met 72) in CaM have been shown to be involved in hydrophobic interactions with a 26-residue MLCK peptide, a fragment from myosin light chain kinase (Ikura et al., 1992; Meador et al., 1992). Thus, it is interesting to speculate that the four N-terminal Met residues in cTnC (Met 45, Met 80, Met 81, and Met 85), which correspond to the N-terminal Met residues involved in MLCK peptide binding in CaM, may be involved in binding the inhibitory peptide derived from TnI. In addition, Met residues 120 and 157 located in the C-terminal domain in cTnC form a hydrophobic surface similar to that formed by Met 109 and Met 144 in CaM. We have utilized the soluble paramagnetic relaxation probe, HyTEMPO, to map the binding site of cTnIp on cTnC.

Results

^{1}H and ^{13}C chemical shifts of the 10 methionine methyl protons of [methyl-^{13}C]Met-labeled cTnC(C35S) were previously assigned in our laboratory by comparison of HSMQC spectra of cTnC3, cTnC(C35S), and a series of six triple mutant and six single mutant proteins where Met residues were systematically changed to Leu (Lin et al., 1994) and used to monitor the binding of cTnI to cTnC (Krudy et al., 1994). In the two-dimensional HSMQC spectrum of Ca^{2+}-saturated [^{13}C-methyl]Met-labeled cTnC(C35S) each of the 10 Met methyl protons were clearly resolved and assigned allowing their use as structural probes (Fig. 1). A monocysteine derivative of recombinant cTnC where Cys 35 was changed to Ser (Putkey et al., 1993) was chosen for this study because, under conditions of the NMR experiment, the C35S mutant does not form disulfide-linked dimers as judged by ^{1}H NMR spectroscopy and native polyacrylamide gel electrophoresis (data not shown).

The environment of each methionine in Ca^{2+}-saturated cTnC was probed by measuring the proton longitudinal relaxation rate, R_1, of its methyl protons. This was done through a set of T_1-HSMQC experiments in which the proton magnetization was inverted along the z-axis by a 180° proton pulse, followed by a variable length delay and then an HSMQC pulse sequence (Petros et al., 1992). The proton longitudinal relaxation rate was obtained by plotting the recovery of proton magnetization along the z-axis versus delay times, τ, in the T_1-HSMQC sequence. Figure 1 shows T_1-HSMQC spectra of Ca^{2+}-saturated [^{13}C-methyl]Met-labeled cTnC(C35S) having delay times, τ, of 0, 0.9, and 1.3 s, respectively. The magnitude of the recovered proton magnetization was obtained from the volume of the assigned cross peak in the T_1-HSMQC spectra and exponential fits of these volumes provided values for R_1 (Table 1). Figure 2 shows typical T_1 plots for Met 47 in the N-terminal domain, as well as Met 103 and Met 157 in the C-terminal domain of Ca^{2+}-saturated cTnC(C35S).

The relative solvent exposure of each methyl proton in Ca^{2+}-saturated cTnC(C35S) was determined by remeasuring the relaxation rates, R_{1sl}, upon addition of one equivalent of the soluble spin label HyTEMPO (Table 1; Fig. 2). Those methyl groups that are solvent exposed will be most affected by addition of soluble spin label. No chemical shift changes were observed upon addition of up to five equivalents of HyTEMPO. In addition, up to a fivefold excess of HyTEMPO did not result in the selective broadening of any of the 10 Met methyl groups beyond detection. In contrast, specific binding of HyTEMPO to apomyoglobin could be easily detected by selective broadening of two aromatic resonances (Cocco & Lecomte, 1994). EPR titrations of HyTEMPO with $2Ca^{2+}$-loaded or Ca^{2+}-saturated cTnC(C35S) were performed to determine if HyTEMPO binds to cTnC(C35S) (Weiner, 1969). Figure 3A shows the EPR spectrum of 0.1 mM free HyTEMPO. No increase in the apparent

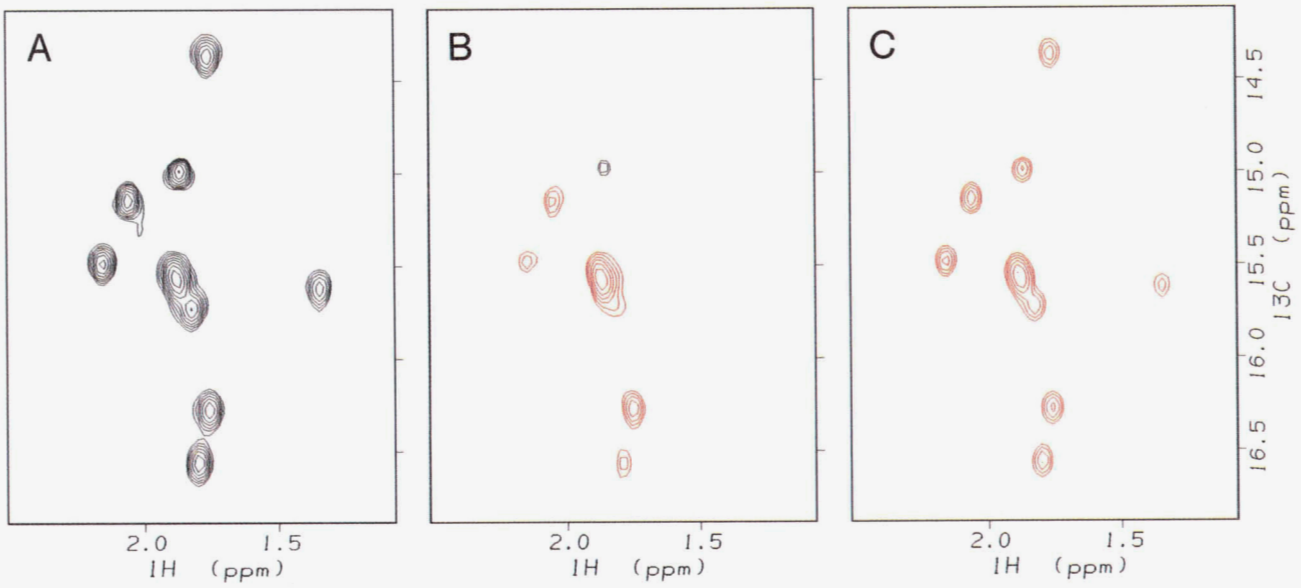

Fig. 1. Contour plots from T_1-HSMQC spectra of Ca^{2+}-saturated cTnC(C35S) in the presence of 1 equivalent of HyTEMPO. Black contours indicate negative peaks and red contours indicate positive peaks. Spectra were acquired with delay times, τ, of **(A)** 0, **(B)** 0.9, and **(C)** 1.3 s. NMR sample was 2 mM [^{13}C-methyl]Met-labeled cTnC(C35S) and 2 mM HyTEMPO in 20 mM Tris-d_{11}, 200 mM KCl, 0.1 mM phenylmethylsulfonyl fluoride in 98% ^2H_2O. Spectra were obtained at 500 MHz and 40 °C as described in the Materials and methods.

Table 1. *[^{13}C-methyl]methionine proton longitudinal relaxation rates for Ca^{2+}-saturated cTnC(C35S) in the presence and absence of HyTEMPO*[a]

Residue	R_1[b] (s^{-1})	R_{1sl}[c] (s^{-1})	$R_{1sl(cTnIp)}$[d] (s^{-1})
45	0.85 ± 0.03	1.26 ± 0.02	1.19 ± 0.03
47	0.84 ± 0.03	2.39 ± 0.24	2.17 ± 0.08
60	0.91 ± 0.02	1.36 ± 0.02	1.27 ± 0.03
80	0.89 ± 0.03	1.17 ± 0.02	1.13 ± 0.04
81	0.82 ± 0.01	1.65 ± 0.04	1.39 ± 0.03
85	0.85 ± 0.02	2.10 ± 0.04	1.81 ± 0.04
103	0.75 ± 0.03	2.08 ± 0.08	1.68 ± 0.08
120	0.86 ± 0.02	2.25 ± 0.08	1.52 ± 0.03
137	0.90 ± 0.02	1.36 ± 0.02	1.24 ± 0.03
157	0.79 ± 0.03	3.96 ± 0.27	2.05 ± 0.10

[a] R_1 is the longitudinal relaxation rate for each of the methyl Met protons of Ca^{2+}-saturated cTnC(C35S) calculated from an exponential fit of the measured ^1H–^{13}C cross-peak volumes from seven T_1-HSMQC experiments with different τ values. R_{1sl} is the calculated longitudinal relaxation rate for each of the methyl Met protons of cTnC(C35S) in the presence of HyTEMPO. $R_{1sl(cTnIp)}$ is the calculated longitudinal relaxation rate for each of the methyl Met protons of Ca^{2+}-saturated cTnC(C35S) in the presence of HyTEMPO and cTnIp. Errors in R_1 represent errors in the exponential fit of the cross-peak intensities. T_1-HSMQC experiments were obtained at 500 MHz in 20 mM Tris-d_{11}, pH 7.5, containing 200 mM KCl at 40 °C.

[b] The sample contained 2 mM Ca^{2+}-saturated cTnC(C35S).

[c] The sample contained 2 mM Ca^{2+}-saturated cTnC(C35S) and in 2 mM HyTEMPO.

[d] The sample contained 2 mM Ca^{2+}-saturated cTnC(C35S), 2 mM HyTEMPO, and 2 mM cTnIp.

anisotropy of the EPR signal intensity of HyTEMPO was observed upon addition of either 1.3 equivalents of $2Ca^{2+}$-loaded cTnC(C35S) (Fig. 3B) or Ca^{2+}-saturated cTnC(C35S) (Fig. 3C), demonstrating that the spin label is not immobilized by the protein (Fig. 3). Specific or nonspecific binding of HyTEMPO to cTnC(C35S) would have resulted in an increased anisotropy of the EPR signal. Taken together, these data demonstrate that specific interactions between HyTEMPO and cTnC(C35S) are unlikely, making HyTEMPO a useful probe for detecting solvent-exposed residues in cTnC.

Binding of the 21-amino acid troponin I inhibitory peptide, cTnIp, to Ca^{2+}-saturated cTnC(C35S) would be expected to protect those Met methyl groups in the binding pocket from exposure to the spin label. The addition of cTnIp was found to most significantly decrease the effect of HyTEMPO on the relaxation rates of the methyl groups of Met 120 and Met 157, qualitatively demonstrating that these resonances are less solvent exposed in the presence of the inhibitory peptide (Table 1; Fig. 2).

Quantitatively, the paramagnetic contribution of the spin label to the observed R_1 is determined from the paramagnetic effect on the relaxation rate, R_{1p}, by

$$R_{1p} = R_{1sl} - R_1,$$

where R_1 is the diamagnetic relaxation rate and R_{1sl} the relaxation rate in the presence of HyTEMPO. The magnitude of the paramagnetic effect, R_{1p}, is related to a measure of relative solvent exposure of each Met methyl group. Calculated R_{1p} values for the 10 Met methyl groups in Ca^{2+}-saturated cTnC(C35S) are given in Table 2. Under some conditions, in the presence of

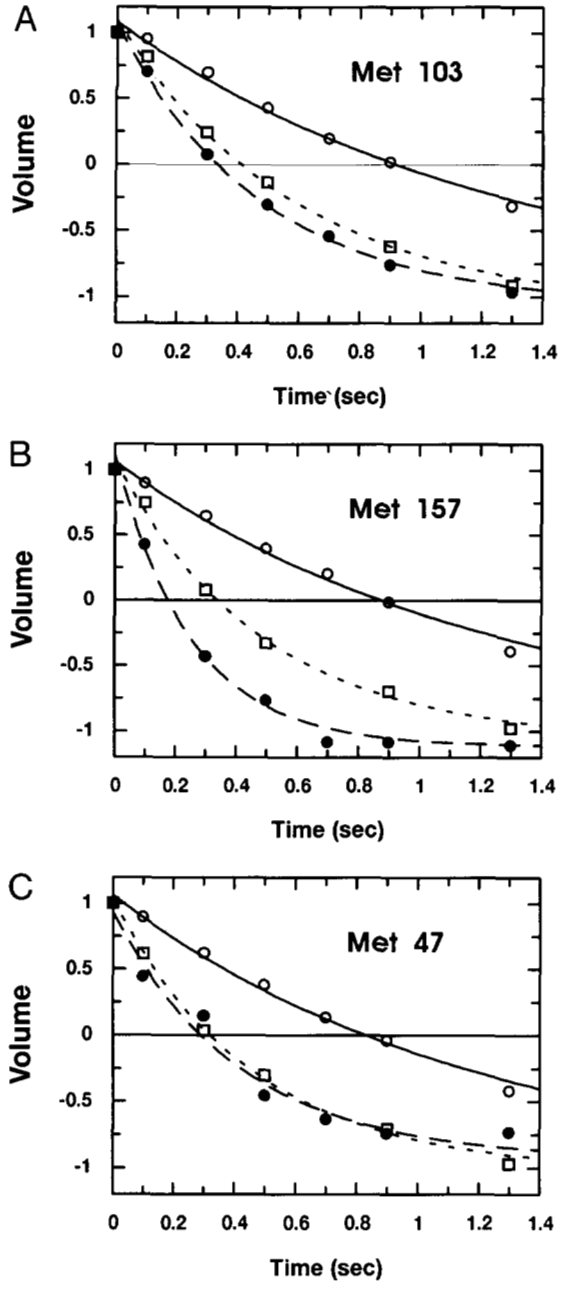

Fig. 2. Proton longitudinal relaxation rates for the Met methyl groups of cTnC(C35S) were determined from the exponential fit of the cross-peak intensities measured from a series of T_1-HSMQC spectra. Exponential fits of the cross-peak intensities are shown for **(A)** Met 103 and **(B)** Met 157, in the C-terminal domain, and **(C)** Met 47, in the N-terminal domain, of 2 mM Ca^{2+}-saturated cTnC(C35S) in the absence of HyTEMPO (○), in the presence of 2 mM HyTEMPO (●), and in the presence of 2 mM HyTEMPO and 2 mM cTnIp (□). Spectra were obtained as described in Figure 1.

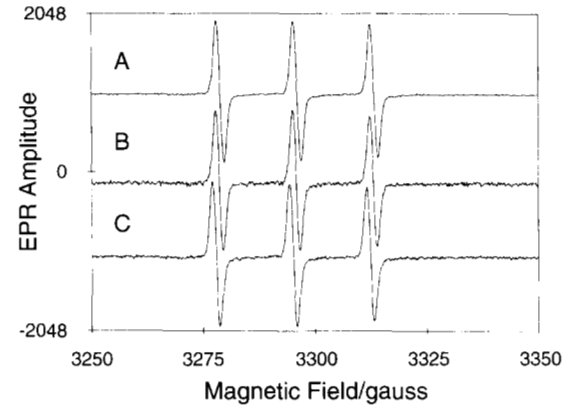

Fig. 3. EPR spectra of HyTEMPO free and in the presence of $2Ca^{2+}$-loaded cTnC(C35S) and Ca^{2+}-saturated cTnC(C35S). EPR spectra were obtained on **(A)** 0.1 mM HyTEMPO, **(B)** 0.1 mM HyTEMPO in the presence of 0.13 mM $2Ca^{2+}$-loaded cTnC(C35S), and **(C)** 0.1 mM HyTEMPO in the presence of 0.13 mM Ca^{2+}-saturated cTnC(C35S) in 20 mM Tris, pH 7.5, containing 200 mM KCl. Spectra were obtained as described in the Materials and methods.

higher concentrations of HyTEMPO, the ^1H-^{13}C correlations for Met 60 and Met 137 become partially overlapping. In cases where the ^1H-^{13}C correlations partially overlapped, R_1 values were measured by centering the integration box precisely at the chemical shift values for Met 60 and Met 137 in the absence of spin label. This allowed a reasonable estimate of R_{1sl} and R_{1p} values for Met 60 and 137 at higher HyTEMPO concentrations. Methionines 45, 60, 80, and 137 exhibit small R_{1p} values, suggesting that their methyl groups are relatively inaccessible to HyTEMPO and hence solvent. From the magnitude of paramagnetic effects, methyl groups of Met 47, 81, 85, 103, 120, and 157 are all partially exposed to the spin label and hence solvent (Table 2). The largest R_{1p} value was found for Met 157, suggesting that its methyl group is the most solvent exposed (Ta-

Table 2. *[^{13}C-methyl]methionine protection ratios for Ca^{2+}-saturated cTnC(C35S) complexed with cTnI peptide*[a]

Residue	R_{1p} (s^{-1})	$R_{1p(cTnIp)}$ (s^{-1})	$R_{1p(cTnIp)}/R_{1p}$
45	0.41 ± 0.04	0.34 ± 0.04	0.83 ± 0.13
47	1.55 ± 0.24	1.33 ± 0.09	0.86 ± 0.15
60	0.45 ± 0.03	0.36 ± 0.04	0.80 ± 0.10
80	0.28 ± 0.04	0.24 ± 0.05	0.86 ± 0.22
81	0.83 ± 0.04	0.57 ± 0.03	0.69 ± 0.05
85	1.25 ± 0.04	0.96 ± 0.04	0.77 ± 0.04
103	1.33 ± 0.09	0.93 ± 0.09	0.70 ± 0.08
120	1.39 ± 0.08	0.66 ± 0.09	0.47 ± 0.07
137	0.46 ± 0.03	0.34 ± 0.04	0.74 ± 0.10
157	3.17 ± 0.27	1.26 ± 0.10	0.40 ± 0.05

[a] R_{1p} is the paramagnetic contribution to the relaxation rate and is equal to $R_{1sl} - R_1$. $R_{1p(cTnIp)}$ is the paramagnetic contribution to the relaxation rate in the presence of cTnIp and is equal to $R_{1sl(cTnIp)} - R_1$. Errors in R_{1p} and $R_{1p(cTnIp)}$ are probable deviations of the difference in R_1 values used to calculate the paramagnetic effect on the relaxation rates. $R_{1p(cTnIp)}/R_{1p}$ is the ratio of the paramagnetic effect on the longitudinal relaxation rate of the methyl group proton in the presence of cTnIp to the paramagnetic effect on the longitudinal relaxation rate of the methyl group proton in the absence of cTnIp. Errors in $R_{1p(cTnIp)}/R_{1p}$ were calculated as the absolute deviation of the quotient.

ble 2). If we make the assumption that Met 157 is fully solvent exposed, then we can estimate that the methyl groups of Met residues 45, 60, 80, and 137 are approximately 12% solvent exposed and the methyl groups of Met residues 47, 85, 103, and 120 are approximately 43% exposed to solvent. The methyl group of Met 81, located near the N-terminus of the central helix, would be approximately 26% solvent exposed.

The binding site on cTnC for the cTnI inhibitory peptide, cTnIp, was mapped by measuring the change in relaxation rates, $R_{1p(TnIp)}$, of the Met methyl protons in the presence of one equivalent of cTnIp (Table 2). From the ratio of $R_{1p(TnIp)}/R_{1p}$, the degree of protection from exposure to HyTEMPO for each Met methyl group upon TnIp binding can be determined (Table 2). Ratios significantly less than 1 indicate protection of the residue by the inhibitory peptide. The ratio $R_{1p(TnIp)}/R_{1p}$ for Met 60 (Table 2) provides a control because, based on the crystal structure of sTnC (Herzberg & James, 1985; Herzberg et al., 1986) and model building of cTnC (Brito et al., 1991), this Met methyl group is largely buried within the N-terminal hydrophobic core and should be reasonably inaccessible to solvent and HyTEMPO. Based on the $R_{1p(TnIp)}/R_{1p}$ ratios, Met residues 45, 47, 60, 80, and 85 are not significantly protected from the soluble spin label by addition of cTnIp (Table 2). The inhibitory peptide was found to provide only minimal protection from HyTEMPO to Met residues 81, 103, and 137 (Table 2). In contrast, the methyl groups of Met 120 and Met 157 were shown to be significantly protected by addition of cTnIp to Ca^{2+}-saturated cTnC(C35S) (Table 2). Methionine residues 120 and 157 are located in the C-terminal domain of cTnC (Fig. 4; Kinemage 1).

These experiments were repeated on the $2Ca^{2+}$-loaded form of cTnC(C35S) having Ca^{2+} bound only at the C-terminal domain high-affinity sites III and IV. The $2Ca^{2+}$-loaded form of cTnC(C35S) was obtained by titrating apo-cTnC(C35S) with Ca^{2+} while monitoring HSMQC spectra until both high-affinity sites were filled (data not shown). Longitudinal relaxation rates of $2Ca^{2+}$-loaded cTnC(C35S) in the presence and absence of cTnIp, before and after addition of one equivalent of HyTEMPO, are given in Table 3. Table 4 gives the paramagnetic contribution of the spin label on the relaxation rates, R_{1p}, of each Met methyl group. As expected from the relaxation rates, the protection ratios ($R_{1p(TnIp)}/R_{1p}$) show that Met 120 and 157 are most shielded from the soluble spin label by the binding of cTnIp (Table 4). In the $2Ca^{2+}$-loaded form of cTnC, cTnIp fails to provide significant protection from the soluble spin label for any of the remaining Met residues, except Met 81, for which partial protection is again observed (Table 4). The inhibitory peptide, cTnIp, provides the same relative degree of protection from HyTEMPO to Met residues 81, 120, and 157 in both the $2Ca^{2+}$-loaded and Ca^{2+}-saturated forms of cTnC(C35S) (Tables 2, 4). Thus, comparison of the accessibility of the soluble spin label to the Met methyl groups in the $2Ca^{2+}$-loaded and Ca^{2+}-saturated cTnC(C35S)–cTnIp complexes suggests that both forms of cTnC bind the inhibitory peptide in a similar manner (Tables 2, 4; Fig. 4; Kinemages 1, 2).

Paramagnetic contributions to the relaxation rates of Ca^{2+}-saturated and $2Ca^{2+}$-loaded cTnC(C35S) can be used to examine conformational changes that occur when Ca^{2+} binds to site II, the site responsible for triggering muscle contraction. In order to obtain accurate $R_{1p(Ca^{2+}sat)}$ and $R_{1p(2Ca^{2+})}$ values, three separate experiments were performed for both the $2Ca^{2+}$-loaded and Ca^{2+}-saturated forms of cTnC(C35S). This was necessary because separate samples had to be used to obtain $R_{1p(Ca^{2+}sat)}$ and $R_{1p(2Ca^{2+})}$ values. Six identical apo-cTnC(C35S) samples were prepared, from the same protein stock, and Ca^{2+} added to give three $2Ca^{2+}$-loaded and three Ca^{2+}-saturated cTnC(C35S) samples. In previous experiments, a single sample could be used to provide all of the necessary relaxation rate data. Values of $R_{1p(Ca^{2+}sat)}$ and $R_{1p(2Ca^{2+})}$ given in Table 5 are average values from the individual experiments.

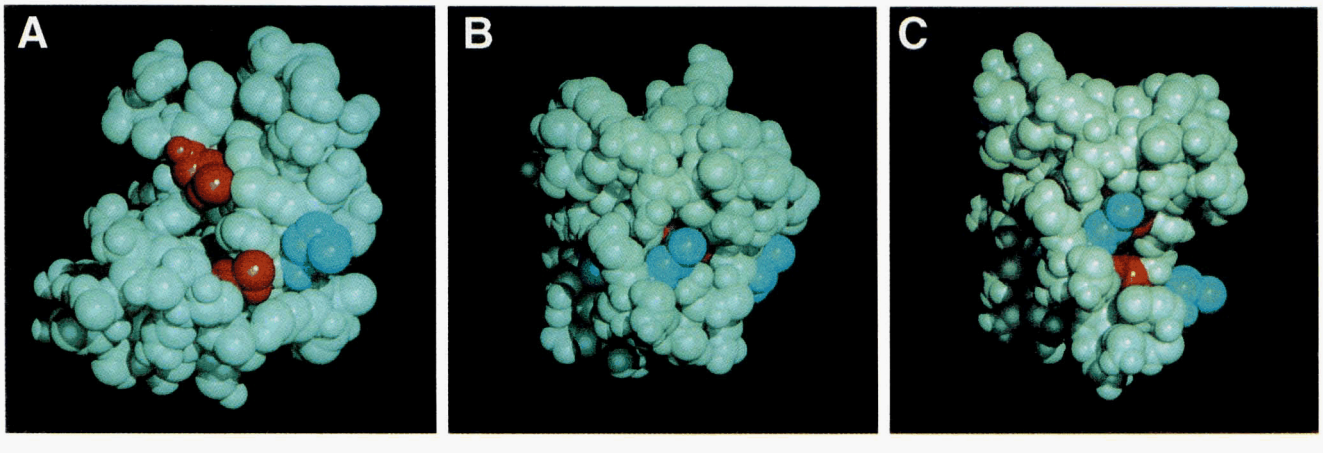

Fig. 4. Backbone representation of the models for cTnC (Brito et al., 1991) highlighting the Met side chains. Methionine methyl groups that do not show a significant change in solvent exposure are shown in blue. Methionine methyl groups showing a significant change in solvent exposure are shown in red. **A:** C-terminal domain of cTnC showing Met 120 and Met 157 is in red. Only Met 120 and Met 157 are significantly protected from solvent by the binding of cTnIp. **B:** N-terminal domain of $2Ca^{2+}$-loaded cTnC. Methionines 45 and 81, which become more solvent exposed with Ca^{2+} binding to the N-terminal regulatory site, are shown in red. **C:** N-terminal domain of Ca^{2+}-saturated cTnC showing the increased solvent exposure of Met residues 45 and 81. Methionine residues 45 and 81 are shown in red.

Table 3. *[^{13}C-methyl]methionine proton longitudinal relaxation rates for 2Ca^{2+}-loaded cTnC(C35S) in the presence and absence of HyTEMPO*[a]

Residue	R_1[b] (s^{-1})	R_{1sl}[c] (s^{-1})	$R_{1sl(cTnIp)}$[d] (s^{-1})
45	0.86 ± 0.03	1.09 ± 0.02	1.14 ± 0.03
47	0.89 ± 0.02	2.34 ± 0.08	2.43 ± 0.08
60	0.98 ± 0.03	1.37 ± 0.04	1.39 ± 0.04
80	0.98 ± 0.03	1.20 ± 0.03	1.15 ± 0.03
81	0.90 ± 0.01	1.41 ± 0.05	1.25 ± 0.04
85	0.90 ± 0.02	2.01 ± 0.05	1.90 ± 0.04
103	0.79 ± 0.02	2.04 ± 0.10	1.91 ± 0.07
120	1.01 ± 0.03	2.68 ± 0.11	1.89 ± 0.06
137	1.02 ± 0.03	1.46 ± 0.04	1.39 ± 0.04
157	0.94 ± 0.03	4.03 ± 0.25	2.38 ± 0.11

[a] R_1 is the longitudinal relaxation rate for each of the methyl Met protons of 2Ca^{2+}-loaded cTnC(C35S) calculated from an exponential fit of the measured ^{1}H-^{13}C cross-peak volumes from seven T_1-HSMQC experiments with different τ values. R_{1sl} is the calculated longitudinal relaxation rate for each of the methyl Met protons of cTnC(C35S) in the presence of HyTEMPO. $R_{1sl(cTnIp)}$ is the calculated longitudinal relaxation rate for each of the methyl Met protons of 2Ca^{2+}-loaded cTnC(C35S) in the presence of HyTEMPO and cTnIp. T_1-HSMQC experiments were obtained at 500 MHz in 20 mM Tris-d_{11}, pH 7.5, containing 200 mM KCl at 40 °C.

[b] The sample contained 2 mM 2Ca^{2+}-loaded cTnC(C35S).

[c] The sample contained 2 mM 2Ca^{2+}-loaded cTnC(C35S) and in 2 mM HyTEMPO.

[d] The sample contained 2mM 2Ca^{2+}-loaded cTnC(C35S), 2 mM HyTEMPO, and 2 mM cTnIp.

Table 4. *[^{13}C-methyl]methionine protection ratios for 2Ca^{2+}-loaded cTnC(C35S) complexed with TnI peptide*[a]

Residue	R_{1p} (s^{-1})	$R_{1p(cTnIp)}$ (s^{-1})	$R_{1p(cTnIp)}/R_{1p}$
45	0.23 ± 0.04	0.28 ± 0.04	1.22 ± 0.27
47	1.45 ± 0.08	1.54 ± 0.08	1.06 ± 0.08
60	0.39 ± 0.05	0.41 ± 0.05	1.05 ± 0.19
80	0.22 ± 0.04	0.17 ± 0.04	0.77 ± 0.23
81	0.51 ± 0.05	0.35 ± 0.04	0.69 ± 0.10
85	1.11 ± 0.05	1.00 ± 0.04	0.90 ± 0.05
103	1.25 ± 0.10	1.12 ± 0.07	0.90 ± 0.09
120	1.67 ± 0.11	0.88 ± 0.07	0.53 ± 0.06
137	0.44 ± 0.05	0.37 ± 0.05	0.84 ± 0.15
157	3.09 ± 0.25	1.44 ± 0.11	0.47 ± 0.05

[a] R_{1p} is the paramagnetic contribution to the relaxation rate and is equal to $R_{1sl} - R_1$. $R_{1p(cTnIp)}$ is the paramagnetic contribution to the relaxation rate in the presence of cTnIp and is equal to $R_{1sl(cTnIp)} - R_1$. Errors in R_{1p} and $R_{1p(cTnIp)}$ are probable deviations of the difference in R_1 values used to calculate the paramagnetic effect on the relaxation rates. $R_{1p(cTnIp)}/R_{1p}$ is the ratio of the paramagnetic effect on the longitudinal relaxation rate of the methyl group proton in the presence of cTnIp to the paramagnetic effect on the longitudinal relaxation rate of the methyl group proton in the absence of cTnIp. Errors in $R_{1p(cTnIp)}/R_{1p}$ were calculated as the absolute deviation of the quotient.

Ratios, $R_{1p(Ca^{2+}sat)}/R_{1p(2Ca^{2+})}$, significantly greater than 1 identify Met methyl groups that become more exposed to HyTEMPO and therefore solvent with the binding of Ca^{2+} to the N-terminal regulatory site. From the average ratios given in Table 5, $R_{1p(Ca^{2+}sat)}/R_{1p(2Ca^{2+})}$, both Met 45 and 81 show a significant increase in exposure to spin label upon Ca^{2+} binding at site II. Based on a model of cTnC (Brito et al., 1991), Met 45 and 81 are located at the base of the proposed hydrophobic cleft in the Ca^{2+}-saturated form of cTnC (Fig. 4; Kinemage 3). Again, assuming that Met 157 is fully exposed, this represents an increase in exposure from 7% to 13% for Met 45 and and increase in exposure from 14% to 26% for Met 81. This is consistent with the solvent accessibility changes for Met 46 and Met 82 in sTnC, corresponding to Met 45 and Met 81 in cTnC, which showed that Met 82 is about twice as exposed to solvent in the Ca^{2+}-saturated form of sTnC as is Met 46 (Herzberg et al., 1986). The magnitude of the opening of the hydrophobic cleft is difficult to predict based on solvent exposure because both residues are located in a pocket (Kinemage 3). Even with one face of the methyl group fully exposed, increases in relaxation rates would not be as great as observed for a fully exposed methyl group having all six possible sides exposed to solvent. The relative accessibility of HyTEMPO for the Met methyl groups of Met 45 and 81 in cTnC is at least consistent with the model. Methionine residues 47, 60, 80, and 85 located in the N-terminal domain of cTnC show no significant change in exposure to HyTEMPO upon Ca^{2+} binding at site II (Table 5). As expected, methionine groups in the C-terminal domain of cTnC were largely unaffected by Ca^{2+} binding at site II (Table 5).

Discussion

TnC and CaM are members of the well-known helix-loop-helix or EF hand family of Ca^{2+} binding proteins (Kretsinger, 1980). The solution structure of the CaM–MLCK peptide complex suggests importance of Met residues in its interaction with the MLCK peptide (Ikura et al., 1992; Meador et al., 1992). Recombinant cardiac troponin C, cTnC3, has 10 Met residues distributed throughout both N- and C-terminal domains. Based on the homology with CaM, Met residues in cTnC are predicted to be involved in the binding of cTnI and the well-known inhibitory peptide derived from cTnI, cTnIp. In addition, a model for Ca^{2+} activation of TnC, based on the crystal structure of turkey skeletal muscle TnC, predicts increased solvent accessibility of several hydrophobic groups including Met 46, Met 48, and Met 82 upon Ca^{2+} binding to the N-terminal domain (Herzberg et al., 1986). These Met residues correspond to Met 45, Met 47, and Met 81, respectively, in cTnC. In the model of cTnC, based on the crystal structure of sTnC, Met 47 is at least partially exposed to solvent in the absence of bound Ca^{2+} at site II (Brito et al., 1991). In contrast, Met 45 and Met 81 in cTnC are predicted to undergo the largest increase in solvent exposure upon Ca^{2+} binding to the regulatory site.

To both characterize the roles of Met residues in the binding of cTnIp to cTnC and to provide experimental evidence for the proposed increased solvent accessibility of Met residues 45 and 81 upon Ca^{2+} binding to this regulatory site, we utilized a soluble paramagnetic probe, HyTEMPO, to identify surface-exposed Met residues and to map the binding site of cTnIp on

Table 5. *[^{13}C-methyl]methionine protection ratios for 2Ca^{2+}-loaded and Ca^{2+}-saturated cTnC(C35S)*[a]

Residue	$R_{1p(2Ca^{2+})}$ (s^{-1})	$R_{1p(Ca^{2+}sat)}$ (s^{-1})	$R_{1p(Ca^{2+}sat)}/R_{1p(2Ca^{2+})}$
45	0.21 ± 0.03	0.42 ± 0.03	2.00 ± 0.32
47	1.5 ± 0.3	1.6 ± 0.1	1.07 ± 0.22
60	0.35 ± 0.05	0.44 ± 0.03	1.26 ± 0.20
80	0.19 ± 0.03	0.26 ± 0.03	1.37 ± 0.27
81	0.44 ± 0.03	0.85 ± 0.03	1.93 ± 0.15
85	1.24 ± 0.07	1.21 ± 0.06	0.98 ± 0.07
103	1.4 ± 0.1	1.3 ± 0.1	0.93 ± 0.10
120	1.8 ± 0.1	1.4 ± 0.1	0.78 ± 0.07
137	0.39 ± 0.04	0.47 ± 0.04	1.21 ± 0.16
157	3.1 ± 0.3	3.3 ± 0.3	1.06 ± 0.14

[a] $R_{1p(2Ca^{2+})}$ is the paramagnetic contribution to the relaxation rate on 2Ca^{2+}-loaded cTnC(C35S) and is equal to $R_{1sl} - R_1$ for 2Ca^{2+}-loaded cTnC(C35S). $R_{1p(Ca^{2+}sat)}$ is the paramagnetic contribution to the relaxation rate on Ca^{2+}-saturated cTnC(C35S) and is equal to $R_{1sl} - R_1$ for Ca^{2+}-saturated cTnC(C35S). $R_{1p(Ca^{2+}sat)}$ and $R_{1p(2Ca^{2+})}$ values are average values from three separate experiments. Errors in $R_{1p(2Ca^{2+})}$ and $R_{1p(Ca^{2+}sat)}$ are probable deviations of the difference in R_{1p} values used to calculate the average paramagnetic effect on the relaxation rates. $R_{1p(Ca^{2+}sat)}/R_{1p(2Ca^{2+})}$ is the ratio of the paramagnetic effect on the longitudinal relaxation rate of the methyl group proton in the presence of bound Ca^{2+} at site II to the paramagnetic effect on the longitudinal relaxation rate in the absence of bound Ca^{2+} at site II. Errors in $R_{1p(Ca^{2+}sat)}/R_{1p(2Ca^{2+})}$ were calculated as the absolute deviation of the quotient.

cTnC. Both EPR and NMR were used to demonstrate that HyTEMPO does not bind to either the 2Ca^{2+}-loaded or Ca^{2+}-saturated forms of cTnC(C35S) (Fig. 3). To date, only a few examples utilizing paramagnetic agents to map protein surfaces or binding sites have been reported (deJong et al., 1988; Petros & Kopple, 1990; Petros et al., 1990, 1992; Fesik et al., 1991; Cocco & Lecomte, 1994). Results from these studies clearly demonstrate the feasibility, accuracy, and resolution that can be obtained using this methodology.

Binding of the 21-residue peptide corresponding to Asn 129–Ile 149 of cTnI (cTnIp) to either 2Ca^{2+}-loaded or Ca^{2+}-saturated cTnC(C35S) resulted in no significant protection of the Met methyl groups in the N-terminal domain from the soluble paramagnetic probe (Fig. 2; Tables 2, 4). This result strongly suggests that the cTnIp peptide does not interact with any Met methyl groups in the N-terminal domain including those that line the proposed hydrophobic pocket. In support of this, Met residues 45, 60, and 80 in both 2Ca^{2+}-loaded and Ca^{2+}-saturated cTnC(C35S) show small R_{1p} and R_{1p}(cTnIp) values, suggesting that they are essentially inaccessible to spin label in both the absence and presence of the cTnIp (Tables 2, 4). In contrast, Met 47 has relatively large R_{1p} and $R_{1p(cTnIp)}$ values in both 2Ca^{2+}-loaded and Ca^{2+}-saturated cTnC as expected for a residue at least partially solvent exposed (Tables 2, 4).

In the C-terminal domain, methyl groups of Met residues 120 and 157 in both 2Ca^{2+}-loaded and Ca^{2+}-saturated cTnC exhibit significant protection by cTnIp from exposure to HyTEMPO suggesting that cTnIp binds to the same site in the C-terminal domain of both cTnC forms (Tables 2, 4). In support of this finding, identical chemical shift changes were seen upon binding cTnIp to both 2Ca^{2+}-loaded and Ca^{2+}-saturated cTnC(C35S) (data not shown). This result is particularly apparent for Met 157, which, in the absence of cTnIp, has the most solvent-exposed methyl group (Tables 2, 4; Fig. 2). Both Met 120 and Met 157 lie on the same face of the C-terminal domain and provide a hydrophobic surface for peptide interaction (Fig. 4; Kinemages 1, 2). This result corresponds to the previous observation based on ^{1}H chemical shift changes, that sTnIp, an inhibitory peptide corresponding to Gly 104–Arg 115 of sTnI, interacts with Phe and Ile residues in the C-terminal hydrophobic pocket of sTnC (Cachia et al., 1983; Slupsky et al., 1992). Alternatively, binding of cTnIp to a site other than the C-terminal hydrophobic pocket could result in a conformational change that leads to a decrease in solvent exposure for both Met residues 120 and 157. However, this seems unlikely because a conformational change sufficient to protect Met residues 120 and 157 would be expected to alter the solvent accessibility of other Met methyl groups.

A number of other studies have also concluded that TnIp interacts primarily with regions in the C-terminal domain (Lan et al., 1989; Wang et al., 1990; Ngai & Hodges, 1992; Swenson & Frederickson, 1992; Ngai et al., 1994). Fluorescent probes reveal that, although intact sTnI is bound to both the N- and C-terminal domains of sTnC, the inhibitory fragments of sTnI (96–116 and 104–115) interact mainly with the C-terminal domain connecting strand of sTnC (Lan et al., 1989). This is in excellent agreement with our observation that Met 120 and Met 157, both at the outer edge of the hydrophobic pocket in the C-terminal domain of cTnC, are protected by the binding of cTnI peptide. In addition, sTnIp had an identical structure, as determined by TRNOE, when bound to either apo or Ca^{2+}-saturated sTnC (Campbell & Sykes, 1991). The structure of a 12-amino acid peptide analog of the cTnI inhibitory peptide bound to cTnC, having Gly at position 110 (in the skeletal and cardiac isoforms a Pro or Thr, respectively, is found at this position), was found to be α-helical with a bend around the Pro 109–Gly 110 bond similar to that observed for sTnI(104–115) bound to sTnC (Campbell et al., 1992). This structure permits the formation of a hydrophobic face away from the basic residues that form a hydrophilic face (Campbell et al., 1992). The bound structure of the inhibitory peptide appears to preclude it from interacting simultaneously with both the N- and C-terminal domains.

Numerous studies have suggested that sTnIp interacts with both the N- and C-terminal domains of sTnC (Kobayashi et al., 1991; Ngai & Hodges, 1992; Swenson & Frederickson, 1992; Farah et al., 1994). An explanation for these observations is that TnC, like CaM, folds over the peptide such that both domains make contact with the inhibitory peptide. However, small-angle X-ray scattering experiments on TnC complexed with intact TnI and TnIp have shown that TnC is extended in both complexes (Blechner et al., 1992; Olah et al., 1994). Therefore, it seems more likely that TnIp can interact with both domains of TnC under appropriate conditions (Ngai & Hodges, 1992). It is now well known that the N-terminal region of TnI interacts with the C-terminal domain of TnC (Farah et al., 1994; Kobayashi et al., 1994; Krudy et al., 1994). Therefore, it is possible that in the intact TnC-TnI complex, the inhibitory region of TnI interacts weakly with the C-terminal domain of TnC, due to the binding of the N-terminal region of TnI, increasing it's affinity for the N-terminal region of TnC depending on the presence of bound Ca^{2+} at the regulatory sites. The N-terminal region of TnI has

also been suggested to function as a negative effector of TnIp binding (Ngai & Hodges, 1992). Regardless of the actual mechanism occurring in the intact troponin complex, our NMR studies clearly demonstrate that cTnIp binds to the C-terminal domain of cTnC in such a manner that both Met 120 and Met 157 are protected from solvent (Fig. 4; Kinemages 1, 2). In addition, our studies support those of Blechner et al. (1992), suggesting that TnC is relatively extended with TnIp bound.

Comparison of the solvent-exposed Met methyl groups in the $2Ca^{2+}$-loaded and Ca^{2+}-saturated forms of cTnC permits elements of the HMJ model (Herzberg et al., 1986) for Ca^{2+} activation to be probed experimentally. Calcium binding to site II, the site responsible for regulating muscle contraction, is predicted to result in increased solvent exposure for the side-chains of Met residues 45, 80, and 81. Based on the $R_{1p(Ca^{2+}sat)}/R_{1p(2Ca^{2+})}$ ratios (Table 5), Ca^{2+} binding at site II results in increased solvent exposure for the side chains of Met residues 45 and 81 (Fig. 4; Kinemage 3). Methionines 45 and 81 also experience the largest chemical shift change upon Ca^{2+} binding to site II (Lin et al., 1994). Methionine residues 47, 60, 80, and 85 failed to show a significant increase in solvent exposure with Ca^{2+} binding at site II (Table 5). Methionine 81 in sTnC, corresponding to Met 80 in cTnC, was predicted to show little change in solvent accessibility with Ca^{2+} binding (Herzberg et al., 1986), which is consistent with our data for Met 80 (Table 5). This is particularly evident when R_{1p} values for Met 80 and Met 60 are compared (Table 5). Modeling suggests that the side chain of Met 60 is only partially exposed to solvent and makes interactions with aromatic amino acids in the N-terminal hydrophobic core (Brito et al., 1991). Based on R_{1p} values, Met 80 is less solvent exposed than Met 60 in both the $2Ca^{2+}$-loaded and Ca^{2+}-saturated forms of cTnC(C35S). In contrast, Met 48 in the HMJ model for Ca^{2+} activation of sTnC, corresponding to Met 47 in cTnC, was predicted to undergo a relatively large change in solvent accessibility (Herzberg et al., 1986) with Ca^{2+} binding to the N-terminal domain. The predicted large increase in solvent accessibility for Met 47 of cTnC was not observed using HyTEMPO as a probe for solvent exposure (Table 5).

Taken together, observed increases in solvent exposure for side chains of Met 45 and 81 residues in the N-terminal domain of cTnC are consistent with the HMJ model of Ca^{2+} activation of sTnC. However, when all of the experimental data are considered, it is likely that the details of the HMJ model will require further experimental refinement, particularly the degree to which the hydrophobic pocket opens with Ca^{2+} binding (Kinemage 3). Quantitating the degree to which the hydrophobic pocket opens will require high-resolution three-dimensional structures of both the $2Ca^{2+}$-loaded and Ca^{2+}-saturated forms of cTnC and measurement of the change in angle between helical pairs A/D and B/C within the N-terminal domain. However, these studies provide the first experimental evidence on Met accessibility in both the $2Ca^{2+}$-loaded and Ca^{2+}-saturated forms of cTnC.

In summary, we have used a soluble paramagnetic probe, HyTEMPO, to identify solvent-exposed Met methyl groups both in the presence and absence of the cTnIp peptide and Ca^{2+} bound at the regulatory site. We have demonstrated the lack of specific interactions between the spin label probe and $2Ca^{2+}$-loaded and Ca^{2+}-saturated cTnC(C35S). Using this approach, we have shown that the isolated cTnI inhibitory peptide binds to the C-terminal domain of cTnC in such a manner as to protect both Met 120 and Met 157 from exposure to solvent. In addition, Ca^{2+} binding to the regulatory site II results in an increased exposure of Met residues 45 and 81. Although this is generally consistent with the HMJ model of Ca^{2+} activation, the details of the model likely need experimental refinement. This approach is currently being used to extend our studies on the cTnI–cTnC complex (Krudy et al., 1994) to map Ca^{2+}/Mg^{2+}-specific, Ca^{2+}-specific, and metal-independent cTnI binding sites on cTnC using recombinant fragments of cTnI.

Materials and methods

Materials

[^{13}C]methyl L-methionine, deuterium oxide, and Tris-d_{11} were obtained from Cambridge Isotope Laboratories. All other chemicals were of the highest purity available commercially.

Troponin I inhibitory peptide

The 21-residue peptide corresponding to Asn 129–Ile 149 of cTnI was synthesized as the *N*-acetyl and carboxyl amide derivative (*N*-acetyl-N-Q-K-I-F-D-L-R-G-K-F-K-R-P-T-L-R-R-V-R-I-a-mide) by the t-butoxycarbonyl/benzyl solid-phase method using a model 403A (Applied Biosystems) automated peptide synthesizer. The peptide was cleaved, deblocked with HF, and purified by reverse-phase HPLC on a 1 × 10-cm C8 ABI/Brownlee column in 70% acetonitrile using a gradient of 0–100% 0.1% trifluoroacetic acid. Amino acid analysis of the major peak was determined by fast atom bombardment mass spectrometry. Purity was determined to be >95%.

Labeled recombinant proteins

Recombinant cardiac troponin C(C35S) (Putkey et al., 1993) was overexpressed in *Escherichia coli* JM109 (Krudy et al., 1992). [methyl-^{13}C]Met-labeled cTnC(C35S) was obtained by growing the bacteria in an enriched defined medium as previously described (Krudy et al., 1994). Recombinant cTnC(C35S) was purified as described previously by Putkey et al. (1989).

Protein samples for NMR experiments were extensively dialyzed against 50 mM $(NH_4)_2CO_3$, lyophilized, and dissolved in NMR buffer containing 20 mM Tris-d_{11} and 200 mM KCl in 98% ^2H_2O at pH 7.5. For preparation of apoprotein, samples were dialyzed three times against 50 mM $(NH_4)_2CO_3$ containing 5 mM EGTA and 10 mM EDTA, desalted on G-25 column, and lyophilized. Final protein concentrations were 2 mM.

EPR methods

EPR spectra were obtained at 298 K using a Varian E6 spectrometer as follows: modulation amplitude, 1 G; microwave power, 1 mW; microwave frequency, 9.227 GHz. EPR spectra were obtained on 0.1 mM HyTEMPO in the presence or absence or either 0.13 mM $2Ca^{2+}$-loaded or Ca^{2+}-saturated cTnC(C35S) in 20 mM Tris, pH 7.5, containing 200 mM KCl.

NMR methods

HSMQC (Zuiderweg, 1990) spectra of the [^{13}C methyl]Met-labeled proteins were collected with 256 complex data points in the t_2 domain and 150 increments in t_1 at 40 °C. The ^{1}H and ^{13}C spectral widths were 5,556 and 2,000 Hz, respectively. The water resonance was suppressed by continuous irradiation during the relaxation delay. T_1-HSMQC spectra were collected with a pulse sequence consisting of a 180° ^{1}H pulse and a variable relaxation delay followed by an HSMQC experiment. HSMQC spectra were processed with a 90° shifted sine-bell-squared function and zero-filled to 512 points in both t_1 and t_2. ^{1}H and ^{13}C chemical shifts were reported relative to the HDO signal at 4.563 ppm and the methyl carbon of [^{13}C-methyl]Met at 14.86 ppm, respectively. All spectra were processed using the FELIX 2.0 software package (Biosym Technologies, Inc.).

The ^{1}H and ^{13}C assignments for the methyls of methionine residues in cTnC were previously determined from HSMQC spectra of a set of recombinant proteins each with a different Met mutated to Leu (Lin et al., 1994). The longitudinal relaxation rates (R_1) were measured from an exponential fit of the measured cross-peak volumes as a function of delay time in the T_1-HSMQC experiment.

Acknowledgments

This work supported by National Institutes of Health grant HL45724 and Welch grant AU-1144 (to J.A.P.) and by American Heart Association grant AHA 92015340 (to P.R.R.). J.A.P. is the recipient of a Research Career Development Award from the National Institutes of Health. We thank Dr. Graham Palmer of the Department of Biochemistry and Molecular Biology at Rice University for the use of his EPR spectrometer.

References

Babu YS, Bugg CE, Cook WJ. 1988. Structure of calmodulin refined at 2.2 Å resolution. *J Mol Biol 204*:191–204.

Blechner SL, Olah GA, Strynadka NCJ, Hodges RS, Trewhella J. 1992. 4Ca^{2+}-troponin C forms dimers in solution at neutral pH that dissociate upon binding various peptides: Small-angle X-ray scattering studies of peptide-induced structural changes. *Biochemistry 31*:11326–11334.

Brito RMM, Putkey JA, Strynadka NCJ, James MNG, Rosevear PR. 1991. Comparative NMR studies on cardiac troponin C and a mutant incapable of binding calcium at site II. *Biochemistry 30*:10236–10245.

Cachia PJ, Sykes BD, Hodges RS. 1983. Calcium-dependent inhibitory region of troponin: A proton nuclear magnetic resonance study on the interaction between troponin C and the synthetic peptide N$^{\alpha}$-acetyl-[FPhe^{106}]TnI-(104–115) amide. *Biochemistry 22*:4145–4152.

Campbell AP, Sykes BD. 1991. Interaction of troponin I and troponin C. Use of the two-dimensional nuclear magnetic resonance transferred nuclear Overhauser effect to determine the structure of the inhibitory troponin I peptide when bound to skeletal troponin C. *J Mol Biol 222*: 405–421.

Campbell AP, VanEyk JE, Hodges RS, Sykes BD. 1992. Interaction of troponin I and troponin C: Use of the two-dimensional transferred nuclear Overhauser effect to determine the structure of a Gly-100 inhibitory troponin I peptide analog when bound to cardiac troponin C. *Biochim Biophys Acta 1160*:35–54.

Cocco MJ, Lecomte JTJ. 1994. The native state of apomyoglobin described by proton NMR spectroscopy: Interaction with the paramagnetic probe HyTEMPO and fluorescent dye ANS. *Protein Sci 3*:267–281.

Collins JH, Greaser ML, Potter JD, Horn MJ. 1977. Determination of the amino acid sequence of troponin C from rabbit skeletal muscle. *J Biol Chem 252*:6356–6362.

deJong EAM, Claesen CAA, Daemen CJM, Harmsen BJM, Konings RNH, Tesser GI, Hibers CW. 1988. Mapping of ligand binding sites on macromolecules by means of spin-labeled ligands and 2D difference spectroscopy. *J Magn Reson 80*:197–213.

Fesik SW, Gemmecker G, Olejniczak ET, Petros AM. 1991. Identification of solvent-exposed regions of enzyme-bound ligands by nuclear magnetic resonance. *J Am Chem Soc 113*:7080–7081.

Grabarek Z, Tan RY, Wang J, Tao T, Gergely J. 1990. Inhibition of mutant troponin C activity by an intra-domain disulphide bond. *Nature 345*: 132–135.

Herzberg O, James MN. 1985. Structure of the calcium regulatory muscle protein troponin C at 2.8 Å resolution. *Nature 313*:653–659.

Herzberg O, Moult J, James MNG. 1986. A model for the Ca^{2+}-induced conformational transition of troponin C (a trigger for muscle contraction). *J Biol Chem 261*:2634–2638.

Holroyde MJ, Robertson SP, Johnson JD, Solaro RJ, Potter JD. 1980. The calcium and magnesium binding sites on cardiac troponin and their role in the regulation of myofibrillar adenosine triphosphatase. *J Biol Chem 255*:11688–11693.

Ikura M, Clore GM, Gronenborn AM, Zhu G, Klee CB, Bax A. 1992. Solution structure of a calmodulin-target peptide complex by multidimensional NMR. *Science 256*:632–638.

Kobayashi T, Tao T, Gergely J, Collins JH. 1994. Structure of the troponin complex: Implications of photocross-linking of troponin I to troponin C thiol mutants. *J Biol Chem 269*:5725–5729.

Kretsinger RH. 1980. Structure and evolution of calcium-modulated proteins. *CRC Crit Rev Biochem 8*:119–174.

Krudy GA, Kleerekoper Q, Guo X, Howarth JW, Solaro RJ, Rosevear PR. 1994. NMR studies delineating spatial relationships within the cardiac troponin I–troponin C complex. *J Biol Chem 269*:23731–23735.

Krudy GA, Rui MMM, Putkey JA, Rosevear PR. 1992. Conformational changes in the metal-binding sites of cardiac troponin C induced by calcium binding. *Biochemistry 31*:1595–1602.

Lan J, Albaugh S, Steiner RF. 1989. Interactions of troponin I and its inhibitory fragment (residues 104–115) with troponin C and calmodulin. *Biochemistry 28*:7380–7385.

Lin X, Krudy GA, Howarth JW, Rosevear PR, Putkey JA. 1994. Assignment and calcium dependence of methionyl ϵC and ϵH resonances in cardiac troponin C. *Biochemistry 33*:14434–14442.

Meador WE, Means AR, Quiocho FA. 1992. Target enzyme recognition by calmodulin: 2.4 Å structure of a calmodulin–peptide complex. *Science 257*:1251–1254.

Negele JC, Dotson DG, Liu W, Sweeney HL, Putkey JA. 1992. Mutation of the high affinity calcium binding sites in cardiac troponin C. *J Biol Chem 267*:825–831.

Ngai SM, Hodges RS. 1992. Biologically important interactions between synthetic peptides of the N-terminal region of troponin I and troponin C. *J Biol Chem 267*:15715–15720.

Ngai SM, Sönnichsen FD, Hodges RS. 1994. Photochemical cross-linking between native rabbit skeletal troponin C and benzoylbenzoyl-troponin I inhibitory peptide, residues 104–115. *J Biol Chem 269*:2165–2172.

Olah GA, Rokop SE, Wang CL, Blechner SL, Trewhella J. 1994. Troponin I encompasses an extended troponin C in the Ca^{2+}-bound complex: A small-angle X-ray and neutron scattering study. *Biochemistry 33*: 8233–8239.

Petros AM, Kopple KD. 1990. NMR studies of protein surfaces: The interaction of lysozyme with tri-*N*-acetylglucosamine. *Biochem Pharmacol 40*:65–68.

Petros AM, Mueller L, Kopple KD. 1990. NMR identification of protein surfaces using paramagnetic probes. *Biochemistry 29*:10041–10048.

Petros AM, Neri PN, Fesik SW. 1992. Identification of solvent-exposed regions of an FK-506 analog, ascomycin, bound to FKBP using a paramagnetic probe. *J Biomol NMR 2*:11–18.

Putkey JA, Dotson DG, Mouawad P. 1993. Formation of inter- and intramolecular disulfide bonds can activate cardiac troponin C. *J Biol Chem 268*:6827–6830.

Putkey JA, Sweeney HL, Campbell ST. 1989. Site-directed mutation of the trigger calcium-binding sites in cardiac troponin C. *J Biol Chem 264*: 12370–12378.

Robertson SP, Johnson JD, Potter JD. 1981. The time course of Ca^{2+} exchange with calmodulin, troponin, parvalbumin, and myosin in response to transient increases in Ca^{2+}. *Biophys J 34*:559–569.

Rosevear PR. 1988. Purification and NMR studies of [methyl-^{13}C]methionine labeled truncated methionyl tRNA synthetase. *Biochemistry 27*: 7931–7939.

Satyshur KA, Sambhoroa TR, Pyzalska D, Drendael W, Greaser M, Sundaralingam M. 1988. Refined structure of chicken skeletal muscle troponin C in the two-calcium state at 2-Å resolution. *J Biol Chem 263*: 1628–1647.

Slupsky CM, Shaw GS, Campbell AP, Sykes BD. 1992. A ^{1}H NMR study of a ternary peptide complex that mimics the interaction between troponin C and troponin I. *Protein Sci 1*:1595–1603.

Strynadka NCJ, James MNG. 1989. Crystal structures of the helix-loop-helix calcium-binding proteins. *Annu Rev Biochem 58*:951–998.

Sweeney HL, Brito RMM, Rosevear PR, Putkey JA. 1990. The low-affinity Ca^{2+}-binding sites in cardiac/slow skeletal muscle troponin C perform distinct functions: Site I alone cannot trigger muscle contraction. *Proc Natl Acad Sci USA 87*:9538–9542.

Swenson CA, Frederickson RS. 1992. Interaction of troponin C and troponin C fragments with troponin I and the troponin I inhibitory peptide. *Biochemistry 31*:3420–3429.

Taylor DA, Sack JS, Maune JF, Beckingham K, Quiocho FA. 1991. Structure of recombinant calmodulin from *Drosophila melanogaster* refined at 2.2 Å resolution. *J Biol Chem 266*:21375–21380.

VanEerd JP, Takahashi K. 1976. Determination of the complete amino acid sequence of bovine cardiac troponin C. *Biochemistry 15*:1171–1180.

Wang Z, Sarkar S, Gergely J, Tao T. 1990. Ca^{2+}-dependent interactions between the C-helix of troponin-C and troponin-I. *J Biol Chem 265*: 4953–4957.

Weiner H. 1969. Interaction of a spin-labeled analog of nicotinamide-adenine dinucleotide with alcohol dehydrogenase. I. Synthesis, kinetics, and electron paramagnetic resonance studies. *Biochemistry 8*:526–533.

Zot HG, Potter JD. 1982. A structural role for the Ca^{2+}-Mg^{2+} sites on troponin C in the regulation of muscle contraction. *J Biol Chem 257*: 7678–7683.

Zuiderweg ERP. 1990. A proton-detected heteronuclear chemical-shift correlation experiment with improved resolution and sensitivity. *J Magn Reson 86*:346–357.